Bioactive Materials 1 (2016) 132–139

Contents lists available at ScienceDirect

Bioactive Materials

journal homepage: http://www.keaipublishing.com/en/journals/bioactive-materials/

Magnesium incorporated chitosan based scaffolds for tissue engineering applications

Udhab Adhikari [a, d], Nava P. Rijal [b, d], Shalil Khanal [c, d], Devdas Pai [a, d], Jagannathan Sankar [a, d], Narayan Bhattarai [b, d, *]

[a] Department of Mechanical Engineering, North Carolina A&T State University, Greensboro, NC, USA
[b] Department of Chemical, Biological and Bioengineering, North Carolina A&T State University, Greensboro, NC, USA
[c] Department of Energy and Environmental Systems, North Carolina A&T State University, Greensboro, NC, USA
[d] NSF ERC for Revolutionizing Metallic Biomaterials, North Carolina A&T State University, Greensboro, NC, USA

ARTICLE INFO

Article history:
Received 2 May 2016
Received in revised form
11 November 2016
Accepted 14 November 2016
Available online 23 November 2016

Keywords:
Chitosan
Magnesium gluconate
Carboxymethyl chitosan
Tissue engineering
Composite scaffolds

ABSTRACT

Chitosan based porous scaffolds are of great interest in biomedical applications especially in tissue engineering because of their excellent biocompatibility *in vivo*, controllable degradation rate and tailorable mechanical properties. This paper presents a study of the fabrication and characterization of bioactive scaffolds made of chitosan (CS), carboxymethyl chitosan (CMC) and magnesium gluconate (MgG). Scaffolds were fabricated by subsequent freezing-induced phase separation and lyophilization of polyelectrolyte complexes of CS, CMC and MgG. The scaffolds possess uniform porosity with highly interconnected pores of 50–250 μm size range. Compressive strengths up to 400 kPa, and elastic moduli up to 5 MPa were obtained. The scaffolds were found to remain intact, retaining their original three-dimensional frameworks while testing in in-vitro conditions. These scaffolds exhibited no cytotoxicity to 3T3 fibroblast and osteoblast cells. These observations demonstrate the efficacy of this new approach to preparing scaffold materials suitable for tissue engineering applications.

1. Introduction

Tissue defects and diseases due to trauma, injuries, infections, degeneration, and congenital deformity are a major human health concern. These problems underscore the need for improved tissue regeneration treatment technologies. There has been some recent progress in organ transplantation and surgical reconstruction. Smaller sized defects are best treated by surgical reconstruction, using the ability of tissue to regenerate and spontaneously heal over time. Defects larger than a critical size require a scaffold, or substrate, to support the cell growth and guide the repair process. The current clinical approach mostly involves the use of autografts (from the patient's own tissue) and allografts (tissue other than the patient's own). Several considerations limit the use of these techniques: significant morbidity-related complications at the tissue donation site in the body, the unavailability of matching donor tissue, risk of disease transmission and immune rejection [1–3]. Tissue engineering is evolving as a third approach to overcome these limitations and to develop viable grafts. With this approach, new tissue can be regenerated using a synthetic scaffold as a substrate to promote cell adhesion and proliferation. The scaffold material is designed to biodegrade in a controlled fashion, leaving the space for newly formed tissues [3–6]. The repair process can further be aided by loading drugs and growth factors into such scaffolds [3].

The material properties ideally required for tissue regeneration scaffold drive the choice of material. A partial listing of these properties is: uniform porosity with macro as well as micro-sized pores, non-toxicity to the host tissue, biodegradation and bioresorption, and sufficient mechanical properties [7]. Macropores are required for cell and blood vessels to grow and migrate [8], whereas micropores play a vital role in cell-cell communication, and nutrient transport and removal of waste products [9,10]. Most current candidate materials fail to satisfy all the requirements, due either to insufficient strength during implantation, or the inability to degrade at same rate as that of new tissue growth. If the tissues

* Corresponding author. Department of Chemical, Biological and Bioengineering, North Carolina A&T State University, Greensboro, NC, USA.
E-mail address: nbhattar@ncat.edu (N. Bhattarai).
Peer review under responsibility of KeAi Communications Co., Ltd.

http://dx.doi.org/10.1016/j.bioactmat.2016.11.003

are not mechanically stressed sufficiently during the growth stage, they will not be able to bear the physiological stresses of post-treatment use. The composites of biodegradable natural polymers and ceramics come closest to fulfilling most of these property requirements. The organic polymer phase enhances the biodegradation needed to provide the space for tissue growth. The dispersed phase provides the required mechanical integrity to the scaffold [11,12].

Chitosan, made of glucosamine and N-acetylglucosamine units linked by one to four glycosidic bonds, has been proven to be biologically renewable, biodegradable, biocompatible, nonantigenic, nontoxic, biofunctional. Also, it also bears the proxy structure of glycosaminoglycan (GAG), a major component that constitutes the tissue extracellular matrix (ECM) [13–15]. Chitosan and some of its complexes have also been studied for use in a number of other biomedical applications, including wound dressings, drug delivery systems, and space-filling implants [16,17]. However, the major drawback of chitosan is its lack of proper mechanical strength for hard tissue engineering applications. Several studies have been conducted to improve its strength by reinforcing it with various ceramic phases like wollastonite, hydroxyapatite and beta tricalcium phosphate (β-TCP) and also by polyblending with other synthetic and natural polymers [18]. In this study, chitosan was combined with its oppositely-charged derivative, carboxymethyl chitosan (CMC) to form a stable matrix phase and magnesium gluconate (MgG) as the dispersed phase. MgG is an organic salt of magnesium that readily dissolves to release Mg^{++} ions. A number of studies have demonstrated that divalent cations such as Mg^{++}, Ca^{++}, and Mn^{++} play a critical role in tissue remodeling and development [19–21]. The extracellular matrix (ECM) of tissue contains certain domains that bind divalent cations such as Ca^{++}, Mg^{++} and Mn^{++}. These ECM-bound cations modify the integrin affinity to their respective ligands [20,22–24]. In a study performed by *Zreiqat* et al., human bone-derived cells grown on bioceramic substrate modified with divalent cations showed higher expression levels of β1-, α5, α5α1-, and α3β1-integrin receptors, compared to Mg^{++} free substrates [20]. The choice of Mg for use in implants is further motivated by magnesium's excellent biocompatibility, degradation into non-toxic products and its proven use as an essential nutrient for human metabolism [25].

A porous and bioactive scaffolds was fabricated by using a blend mixture of CS, CMC and MgG, and subsequent freezing-induced phase separation and lyophilization. Magnesium gluconate was first introduced into aqueous solution of CMC and mixed the resulted solution with CS solution in acidic pH prior to freezing and lyophilization to obtain the composite the scaffolds. Scaffold morphology was analyzed by SEM, water uptake and retention ability by weighing the amount of water absorbed and retained after centrifugation and cell toxicity using 3T3 fibroblast and osteoblast cells. Mechanical properties of scaffolds were evaluated under compression loading. Additionally, a release study was carried out at different time points using UV-VIS spectrophotometry to quantify the amount of Mg^{++} released from the chitosan-CMC-based composite scaffolds.

2. Materials and methods

2.1. Materials

Chitosan powder (Medium Mw, DD 75–85%) was purchased from Sigma-Aldrich (St. Louis, MO, USA) and carboxymethyl chitosan (CMC) powder (DD 90%) was purchased from Santa Cruz Biotechnology (Dallas, TX, U.S.A.). Magnesium gluconate dihydrate (MgG) was purchased from Pfaltz & Bauer (Waterbury, CT, USA). Glacial acetic acid and sodium hydroxide (NaOH) were purchased from Acros Organics (Morris Plains, NJ, USA). Phosphate buffered saline (PBS) was purchased from Thermo Fisher Scientific (Fair Lawn, NJ, USA). Alamar blue and Xylidyl blue assay kits were obtained from Stanbio Laboratory (Boerne, TX, USA) and Life Technologies (Grand Island, NY, USA) respectively. (3-(4,5-Dimethylthiazol-2-yl)-2,5-diphenyltetrazolium bromide) (MTT) assay kit was obtained from Sigma-Aldrich (Oakville, ON, Canada).

2.2. Fabrication of scaffolds

Chitosan solution and CMC solutions were prepared at concentrations of 2, 4 and 5 wt%. Chitosan was dissolved in 2% acetic acid. CMC was dissolved in deionized (DI) water. The two solutions were thoroughly mixed in a 1:1 wt ratio in a container rotating inside a Thinky planetary centrifugal mixer (Planetary Centrifugal Mixer, ARM-310) for 30 min at 2000 rpm (Fig. 1). After thorough mixing, the material was injected via syringe in 48-well cell culture dishes. The cast material was kept at 4 °C for about 30 min, transferred to −20 °C for 4 h, and finally to −80 °C for 12 h. The scaffolds were allowed to lyophilize for about 36 h in the freeze dryer (LabConCo, Kansas City, MO). Excess acetic acid in the dried scaffolds was neutralized by immersing the scaffolds in 0.1 M sodium hydroxide (NaOH) solution for 15 min and then washing thrice with DI water.

As in Table 1, two sets of scaffolds were prepared. For the first set of scaffolds, three concentrations of polymer solutions were used, with no added MgG. For the second set of scaffolds, polymer concentration of CS and CMC was held constant at 5% and the relative amount of MgG was varied. The quantity of MgG added to the scaffolds was 5%, 10%–20% of the total weight of the chitosan and CMC dry powder present in the solution. This was done by dissolving the MgG in 2 ml of DI water and then mixing it with the CMC solution. CMC and MgG were allowed to mix in the Thinky mixer for 15 min at 2000 rpm. CS solution was then added to the CMC − MgG system and allowed to crosslink in the Thinky for 30 min at 2000 rpm. The process of casting, freezing, lyophilization and neutralization was repeated similarly. To measure the required weight (W) of MgG in grams, the following equation was used.

$$W_{MgG} = \frac{\%MgG}{100} * [C_1 * V_1 + C_2 * V_2] \quad (1)$$

where, C_1 and C_2 are the concentrations in wt% while V_1 and V_2 are the volumes (in ml) of CS and CMC solutions, respectively.

2.3. Study of morphology and pore size distribution

The surface morphology of the scaffolds was studied by scanning electron microscopy (SEM) (Hitachi SU8000, Japan). Thin discs of ~1 mm thickness were cut from the scaffolds using surgical scalpel. The samples were mounted on the holder with double-sided carbon tape and sputter-coated with gold using a Polaron SEM coating system (Quorum Technologies, East Sussex, UK) for 2 min at 15 mA. The SEM images were taken at an accelerating voltage of 2 kV and current of 5 μA. Scaffold pore size distributions were evaluated using Image J software (NIH, Gaithersburg, MD) according to previous method on the SEM images [26]. The scale bar length is measured in pixels. Three different images were analyzed for each scaffold composition.

2.4. Water uptake and retention abilities

Water absorption efficiency was determined as follows: initial

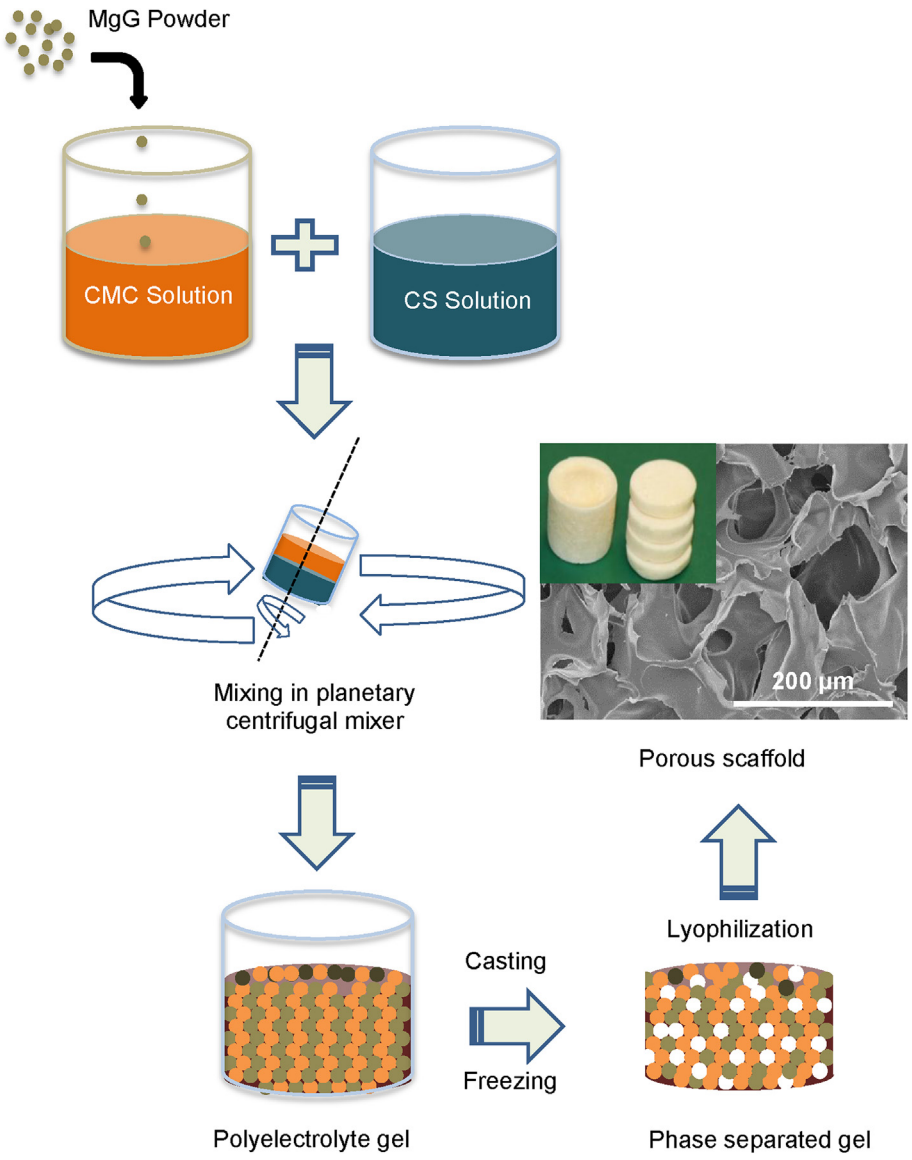

Fig. 1. Schematic flow process showing steps in the fabrication of chitosan scaffolds.

Table 1
Table showing the composition of various scaffolds fabricated.

Sample	Chitosan concentration (wt%) in dil. acetic acid	CMC concentration (wt%) in DI water	Chitosan CMC w ratio	Ratio of chitosan + CMC to MgG
Set A				
A. CS/CMC (2%)	2	2	1:1	NA
B. CS/CMC (4%)	4	4	1:1	NA
C. CS/CMC (5%)	5	5	1:1	NA
Set B				
D. CS/CMC (5%) MgG (5%)	5	5	1:1	1:0.05
E. CS/CMC (5%) MgG (10%)	5	5	1:1	1:0.1
F. CS/CMC (5%) MgG (20%)	5	5	1:1	1:0.2

dry weight (W_d) of the as-prepared scaffold was measured using an electronic balance. The scaffold was neutralized using NaOH to remove any acetate formed during fabrication. It was then immersed in 30 mL DI water at 37 °C for 24 h, after which they were blotted with filter paper to remove excess surface water. The swollen scaffold weight (W_s) was recorded. The equilibrium water absorption ($E_{A,\%}$) was calculated as:

$$E_A = \frac{W_s - W_d}{W_d} X100 \quad (2)$$

The water retention efficiency was determined as follows: the swollen scaffold was transferred to a centrifuge tube with filter paper at the bottom, centrifuged at 500 rpm for 3 min, and then

immediately weighed (W_w). Water retention ($E_{R,\%}$) efficiency of the scaffold at equilibrium was calculated as:

$$E_R = \frac{W_w - W_d}{W_d} X 100 \quad (3)$$

2.5. Mechanical testing

The mechanical testing of the as-prepared scaffolds was performed with an Instron 5542 (Instron Corporation, Canton, MA, USA) using 500 N load cell. After measuring the initial dimensions, the samples were tested for failure under a compressive load. Samples were tested at a displacement rate of 0.5 mm per minute. The test was stopped at 50% reduction in sample height. Load and displacement data collected by the test machine's Merlin software were utilized to compute the strains and the corresponding stress values. These values were plotted using Origin software to obtain the strain-stress graph for individual samples. The failure point in compression was located by using 0.2% offset in the strain value. The stress at this failure point and the slope of the initial linear region were recorded as the compressive stress and compressive modulus.

2.6. Magnesium release study

The magnesium (Mg^{++}) release profile was studied for 5% CS/CMC scaffolds with 5, 10 and 20% MgG concentrations. The release study was carried out by using published protocol of Magnesium Colorimetric Xylidyl Blue Assay (Stanbio Laboratory, Boerne, TX, USA) [27]. The dry weight of each scaffold was measured before neutralizing with NaOH. Neutralized scaffolds were placed in a tube containing 30 ml of 1X PBS solution which was incubated in a Dubnoff Metabolic Shaking Incubator at 37 °C and 30 rpm. 10 μL of fluid was withdrawn from the tube at specified time intervals and added to 1 ml of Xylidyl Blue reagent in a cuvette. After allowing the reagent to react with the sample for 60 min, the absorbance of each sample was measured by a GENESYS 10S UV-VIS Spectrophotometer at 520 nm. The concentration of (Mg^{++}) ions in the solution was calculated from a standard calibration curve previously prepared by using the known concentration of MgG solutions in 1X PBS solution.

2.7. Cell culture and seeding

Scaffolds were cut into 2-mm-thick circular discs and then neutralized with NaOH. Samples were sterilized in 24-well plates by incubating in 95% ethanol for at least 30 min under sterile fume hood. After 30 min, samples were rinsed with sterile DI water twice and 1X DPBS once.

NIH/3T3 cells (a mouse fibroblast cell line) and Osteoblast cells (Homo Sapien bone cell line CRL-11372) were purchased from the American Tissue Type Culture Collection (Manassas, VA). The NIH/3T3 cells were cultured in a 75 cm^2 culture flask with one mL of the growth medium, Dulbecco's modified Eagle's medium (DMEM) (Life Technologies, Grand Island, NY) supplemented with 10% fetal bovine serum (FBS) and 1% antibiotics (10,000 units/mL of penicillin and 10,000 μg/mL of streptomycin) at 37 °C and 5% CO_2. The culture media for osteoblast cells was DMEM supplemented with 10% FBS and 1% Genticin. The culture medium was replaced every 2 days. After reaching about 90% confluence, the cells were detached by 0.025% trypsin and 0.01% EDTA in PBS solution and transferred to centrifuge tube containing culture medium. After centrifugation, the cells were suspended in fresh culture medium and counted using a hemocytometer before seeding to samples. An aliquot of medium containing cells (~50,000 fibroblasts and ~100,000 osteoblasts per samples) was seeded on the scaffold samples (n = 3) and grown in a humidified incubator (37 °C, 5% CO_2) for 72 h.

2.8. Alamar Blue assay

In vitro cytotoxicity was studied by using an Alamar Blue (AB) colorimetric assay (Life Technologies, Grand Island, NY) according to previous publication [6,28]. After 1 and 3 days of incubation, the culture plates were taken out from the incubator and media was removed. Each sample was washed twice with DPBS and incubated with 10% AB containing DMEM supplemented with 10% FBS and 1% antibiotics for 2 h. 1 mL of 10% AB was placed in each well plate. A 400-μL sample of the assay solution was removed from the wells and transferred to an opaque 96-well culture plate for fluorescent measurements on a Spectra max Gemini XPS microplate reader (Molecular Devices, Sunnyvale, CA) at λ_{ex} 530 nm, λ_{em} 590 nm. The relative fluorescent units were converted to a percent of the average values for cells in control wells.

2.9. Cell metabolic activity assay-MTT

The metabolic activity of osteoblast cells when cultured on scaffolds was analyzed by using MTT assay. After 1 and 3 days of incubation, cell seeded scaffolds were transferred into a fresh multi-well plate and 100 μL of fresh medium was added to them. 10 μL of 12 mM MTT solution was added to each well plate and incubated at 37 °C with 5% CO_2 for 4 h. 500 μL of DMSO solution was added to dissolve the precipitated purple colored formazan crystals and the absorbance was recorded at 540 nm by using a Clariostar monochromator microplate reader (BMG Labtech, Ortenberg, Germany).

2.10. Statistical analysis

Each experiment was carried out for $n = 3$. Values are presented as a mean of 3 readings ± standard deviation of these readings. Mean values were compared by one-way analysis of variance (ANOVA). Tukey's *post hoc* test was performed for comparison using Origin software considering $P < 0.05$ to be statistically significant.

3. Results

3.1. Morphology and pore size distribution

Morphology and size distribution of as-synthesized porous 3D scaffolds were assessed by using SEM images (Fig. 2). SEM analysis showed that the scaffolds did have uniform porosity with pore size in the range of 50–150 μm for 4% CS/CMC and 5% CS/CMC scaffolds and 150–250 μm for 2% CS/CMC. Analysis showed that the pore size of 4% CS/CMC and 5% CS/CMC scaffolds were not significantly different at the 0.05 level of statistical significance. However, these two sets of scaffolds showed significantly different pore size range from the 2% CS/CMC scaffolds at the same 0.05 level. For the 5% CS/CMC scaffolds containing 5%, 10% and 20% of MgG, not much difference in the morphology and pore size was observed (Fig. 3). This 100–150 μm pore size range is very beneficial for cell growth [29]. The micrographs also show the small inner pores throughout the structure of the scaffolds. These interconnected pores are required for the cells to communicate freely while the scaffolds are being used for tissue regeneration application.

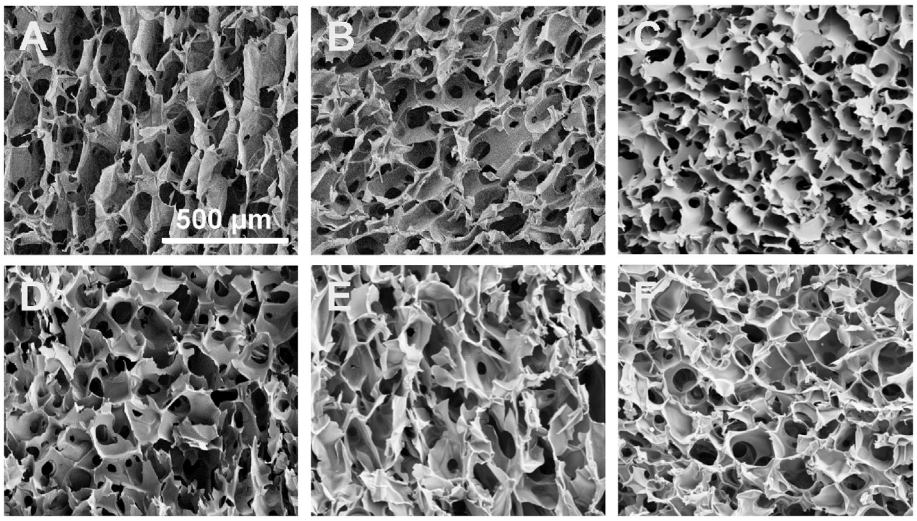

Fig. 2. SEM images A–C: scaffolds containing 2% (A), 4% (B), and 5% (C) of CS/CMC with no MgG; and D–F: 5% CS/CMC containing relative amounts of 5% (D), 10% (E), and 20% (F) MgG respectively. The scale bar represents 500 μm; image taken at 100× magnification.

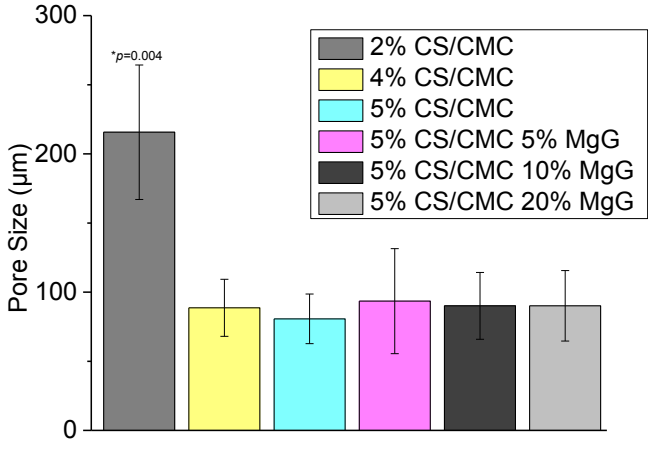

Fig. 3. Pore size distribution of 2, 4 and 5% CS/CMC scaffolds and 5%CS/CMC scaffolds with 5, 10 and 20% MgG respectively. Pore size were determined by Image J software analysis of SEM images ($n = 3$ for each concentration). *$p < 0.05$ compared to 5% CS/CMC with no MgG (sample C on Table 1).

3.2. Water uptake and retention abilities

The water uptake and retention ability of the six types of scaffolds are seen in Fig. 4. Increasing the polymer as well as MgG concentrations lead to a decrease in the degree of water absorption. The water retention ability of CS/CMC scaffolds, however, is seen to increase with increase in the polymer concentration. The water retention ability of 5% CS/CMC scaffolds with no MgG as well as with 5, 10, 20% MgG were found to be comparable, with very slight differences.

3.3. Mechanical properties

The results of the compression test are presented in Fig. 5. The compressive strength of the scaffolds was found to increase from 0.04 MPa to 0.25 MPa (520% increase) as the concentration of CS/CMC polymer was increased from 2 wt% to 5 wt%. Addition of 5% MgG to the 5 wt% CS/CMC scaffold also increased the strength from 0.25 to 0.34 MPa (36% increase). However, there was only a marginal increase in strength of 5 wt% CS/CMC scaffolds from 0.34 to

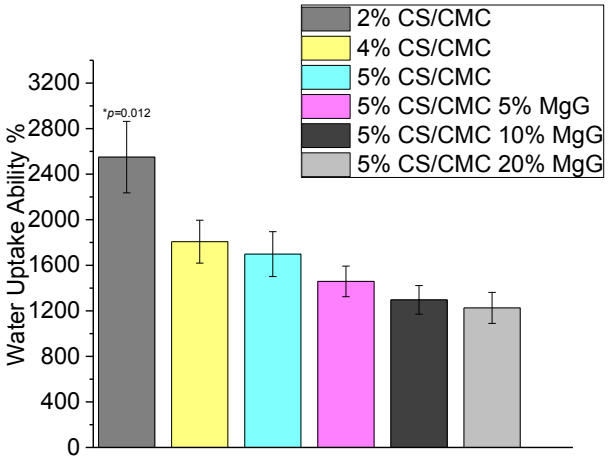

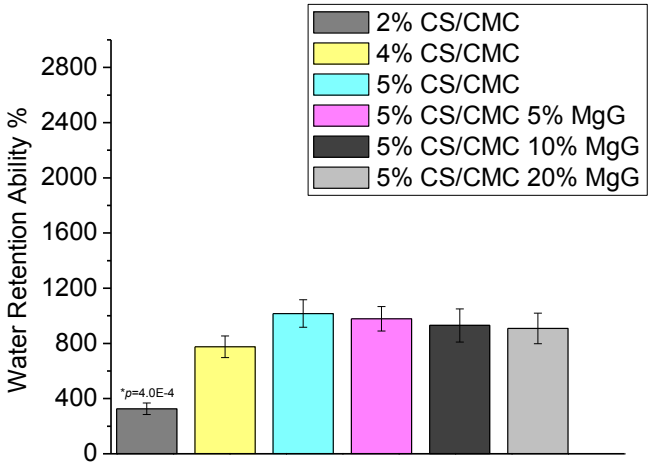

Fig. 4. Water uptake and water retention abilities of 2, 4 and 5%CS/CMC scaffolds and 5%CS/CMC scaffolds with 5, 10 and 20% MgG respectively. The data are presented as the means ± SD ($n = 3$). *$p < 0.05$ compared to 5% CS/CMC.

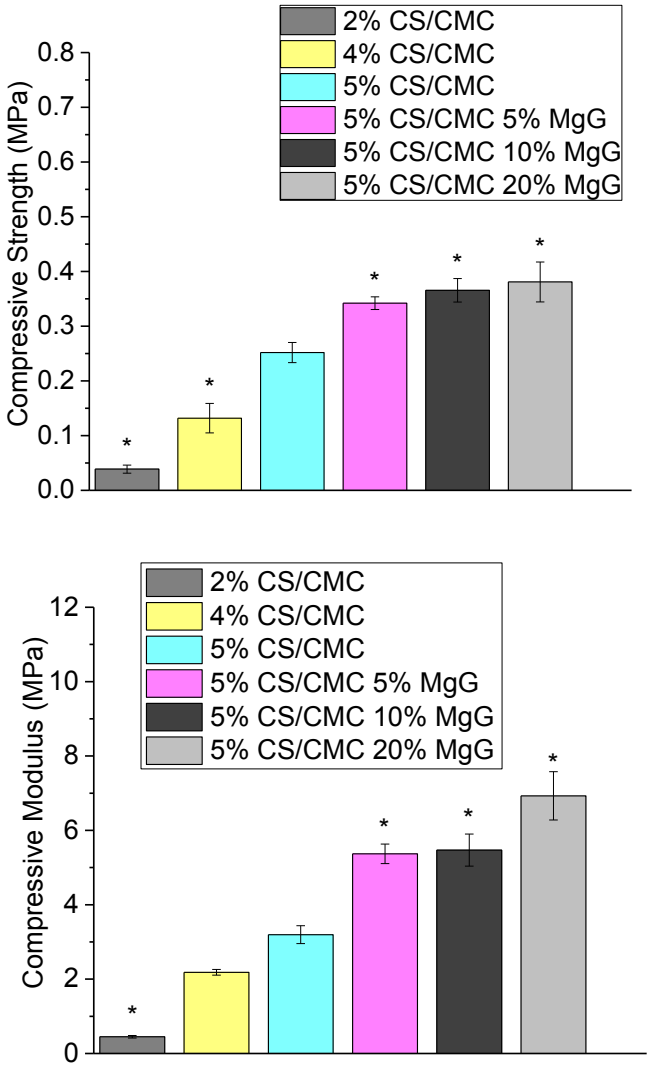

Fig. 5. Compressive strength and compressive modulus 2, 4 and 5%CS/CMC scaffolds and 5%CS/CMC scaffolds with 5, 10 and 20% MgG respectively. The data are presented as the means ± SD ($n = 3$). *$p < 0.05$ compared to 5% CS/CMC.

0.38 MPa (12%) as the relative amount of MgG was increased from 5% to 20%. Similar trends were observed when the compressive modulus of different CS/CMC scaffolds was compared. Compressive modulus was increased from 0.45 MPa to 3.2 MPa (610% increase) when the polymer concentration was increased from 2 wt% to 5 wt % CS/CMC. A further 68% improvement in compressive modulus was observed when 5% MgG was added to 5 wt% CS/CMC scaffolds. There was not much change in the modulus when the amount of MgG was increased to 10% but a sharp increase of 1.6 MPa (30%) in modulus when the MgG amount was increased to 20%.

3.4. Magnesium release study

The magnesium ion (Mg^{++}) release profiles of 5 wt% CS/CMC scaffolds containing 5, 10 and 20% MgG are shown in Fig. 6. The results were obtained in terms of cumulative concentration of magnesium ions at that point in time. Each data point represents the mean of three independent samples. All the scaffolds with different MgG concentrations had similar release profiles. The release profiles of scaffolds showed the sustained release of magnesium ions. The rate of release of magnesium ions from the CS/CMC matrix was initially rapid and then slowed down significantly. No significant differences in magnesium release profile were observed (at the $p < 0.05$ level) between three MgG concentration levels after 154 h. After 154 h, 0.31 mM (70%), 0.57 mM (72%) and 1.3 mM (75%) of Mg^{++} was released from 5%, 10% and 20% MgG scaffolds, respectively.

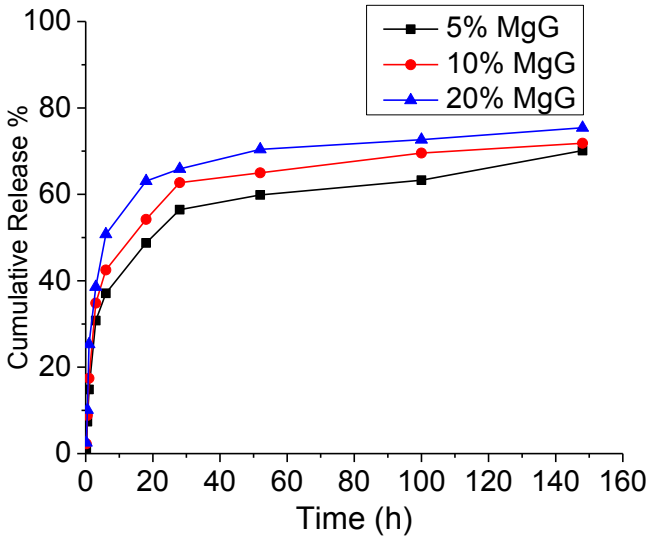

Fig. 6. Cumulative *in vitro* magnesium ions (Mg^{++}) release profile for 5% CS/CMC scaffolds with 5, 10 and 20% relative amounts of MgG. The data are presented as the means ($n = 3$).

3.5. Alamar Blue assay (3T3 fibroblast cells)

Fig. 7 shows the changes in relative levels of AB between 3T3 cells grown on Mg scaffold's surface and on the control substrate (5% CS/CMC (no MgG)). After day 1, the average cell viability for 5% CS/CMC scaffolds with 5, 10 and 20% MgG were found to be 100, 89 and 91% respectively. Similarly, after day 3, these scaffolds exhibited 88, 95 and 90% cell viability respectively as compared to control substrate.

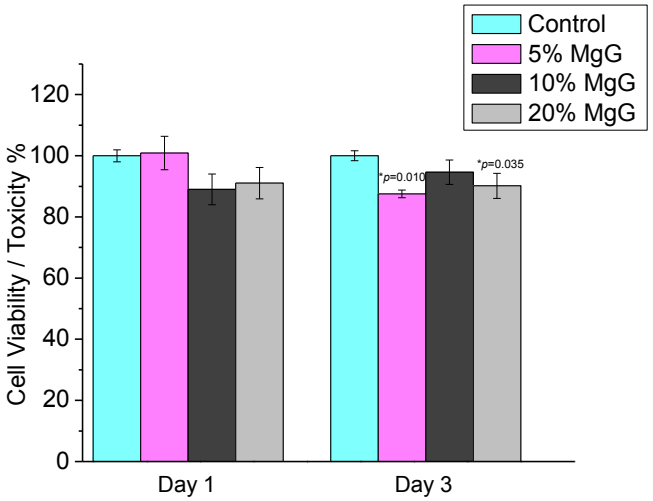

Fig. 7. *In vitro* cytotoxicity for Fibroblast 3T3 cells, a mouse fibroblast cell line in CS/CMC scaffolds with varying amounts of MgG. The data are presented as the means ± SD ($n = 3$). *$p < 0.05$ compared to 5% CS/CMC (no MgG).

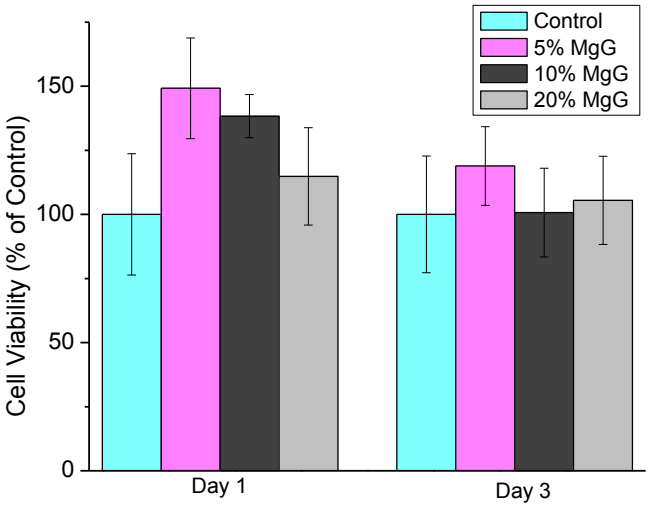

Fig. 8. Relative cell viability for osteoblast cells, a homo sapiens cell line in CS/CMC scaffolds with varying amounts of MgG. The data are presented as the means ± SD ($n = 3$). No statistical significant difference in any groups at $p = 0.05$ compared to 5% CS/CMC (no MgG) was observed.

3.6. Cell metabolic activity assay-MTT

Fig. 8 shows the changes in relative cell viability between osteoblast cells grown on Mg scaffold's surface and on the control substrate (no Mg present). After day 1, the average cell viability for 5% CS/CMC scaffolds with 5, 10 and 20% MgG were found to be 149, 138 and 115% respectively. Similarly, after day 3, these scaffolds exhibited 119, 101 and 101% cell viability respectively as compared to control substrate. The culture media has pH change from 7.36 up to 8.58 and 8.95 after day 1 and 3 respectively (supplementary Table 1). Similar to the results obtained with 3T3 fibroblast cells, cytotoxicity on the Mg-containing scaffold materials were minimal as compared to control substrate which shows that these scaffolds are nontoxic and can provide adequate support for osteoblast cell growth and proliferation.

4. Discussions

Tissue engineering has been widely regarded as an alternative to the traditional autograft and allograft approaches to tissue repair. For successful regeneration of damaged tissue, it is essential to select the proper components to develop a scaffold. Chitosan (CS) is the most-examined among other various available natural polymers, such as alginate, hyaluronic acid, collagen, fibrin, and silk, because of its proven minimal foreign body response, biodegradation into non-toxic products, intrinsic antibacterial nature and low cost [30,31]. In this research, CS was mixed with its negatively-charged derivative CMC to obtain a complex coacervate that, after lyophilization, resulted in a stable scaffold structure. CS and CMC have similar structure but opposite electric charge, which enables them to interact strongly and form polyelectrolyte network structure [32]. Simultaneously, MgG was added in to the mixture of CS and CMC so that MgG-incorporated CS/CMC scaffolds were formed. This is believed to improve osteoblast adhesion properties while it releases divalent Mg^{++} ions in aqueous medium. Overall, through this process, we obtained a bioactive CS/CMC-MgG composite in the form of porous scaffold.

The composite scaffolds developed in this study have pore size of 50–250 μm. These pores were highly interconnected with 3D porous network structures (supplementary Fig. 1). The porous structure of the CS/CMC based composite scaffolds was achieved through a process of thermally-induced phase separation and subsequent sublimation of the solvent. This porous structure allows the passage of nutrients and metabolites as well as provides sites for cell attachment and proliferation [32,33].

During the early stages of the scaffold implantation, it is essential for the scaffold to absorb physiological fluids and the nutrients for consumption by the colonizing osteoblast cells [34]. Hence in the process of developing a tissue engineered scaffold, the water absorption and retention capacities are important factors. The results of water uptake and retention studies suggested that the scaffolds in the present study had the capacity to retain more water than their own weight, as both values were more than 100%. Both the hydrophilic nature of CS and its ability to maintain a 3D structure contribute to the swelling abilities of these scaffolds.

An ideal tissue engineering scaffold should be biocompatible and highly porous and have adequate mechanical properties. The mechanical properties of the synthetic material should be close to those of the target tissue in order to avoid the stress-shielding effect. This allows the scaffold to maintain structural integrity in both *in vivo* and *in vitro* applications. Mechanical properties also influence some of the specific tissue functions within an engineered tissue [35]. The major challenge in designing polymer-based scaffolds for tissue engineering is the tradeoff between adequate material porosity and mechanical strength. Both mechanical properties and pore size can be controlled by process parameters such as pre-freezing temperature, cooling rate, concentration and composition of polymer [36,37]. 5% CS/CMC scaffolds with 20% MgG were found to have both the highest compressive strength (0.38 MPa) and highest compressive modulus (6.9 MPa) among the scaffolds studied. Compressive strength of natural hard tissue like cancellous bone is (1–12) MPa. When the compressive modulus was calculated, it was observed that polymer composition influences the stiffness. A significantly lower modulus was observed in lower concentration CS scaffolds. This may be due to the difference in porosities and pore size between the scaffolds. A higher pore volume and a larger pore size inside the lower concentration scaffold provide the scaffold with a larger deformable space. Thus, the scaffolds of 5 wt% composition, due to having small pore sizes, are mechanically more desirable. Addition of MgG was found to significantly increase the mechanical properties. However, variation of MgG concentration between 5, 10 and 20% did not yield a significant difference in the mechanical strength. Higher concentration of MgG did not contribute to the overall strength. This is attributed to its interference with the phase separation of CS/CMC solution during scaffold formation.

Magnesium (Mg^{++}) is the fourth most abundant cation in the body and affects many cellular functions including energy metabolism, modulation of signal transduction, biomineralization of bone and tooth, cell proliferation and differentiation. Upon contact with aqueous solutions, the hydrophilic surface of MgG-containing CS/CMC scaffold absorbs water and expands, releasing Mg^{++} ions from these hybrid scaffolds. In this study, over a period of 24 h, 75% (1.3 mM) of magnesium ions was released from the scaffolds. In a recent study by *Jiali Wang* et al., it was reported that for cell types L929 and osteoblast, 35 mM and for BMSCs and MC3T3-E1, 15 mM of Mg ion concentrations could be considered to be the critical dose without inhibiting cell viability [38]. In other studies, Mg ions have also been demonstrated to promote cell viability, differentiation, migration and stimulate gene expressions [39,40]. The release profiles contained two distinct regions: the first being burst release and the second, relatively constant release rate, after the initial burst. The hydrophilic nature of CS/CMC, allows permeation of water into the polymer matrix, and diffuses the Mg^{++} ions from scaffolds. Bulk-eroding polymers are often characterized by a burst of drug release during the first few hours of incubation, followed by

a slow, diffusion-controlled release [41]. To obtain a sustained release of Mg^{++} at a constant concentration from the surface of scaffolds for a longer duration, an optimized polymer/MgG composition and scaffold preparation technique will be needed.

The cell viability of these scaffold materials were assessed by using a previously-established Alamar Blue (AB) as well as MTT assay [28]. Comparison with cell viability on a control substrate provides a relative measure of cell number. According to the current ISO standards of Part 5, cell viability higher than 75% could be considered with no toxic risks for medical devices, so we defined the Mg^{++} ions concentration with 75% cell viability as the safety level in our experiment [38]. All of the samples with MgG in this experiment showed cell viability greater than 75% with 3T3 fibroblast cells. The same scaffolds showed metabolic activities greater than 100% with osteoblast cells.

5. Conclusions

Chitosan-magnesium-based composite scaffolds were successfully synthesized. The scaffold properties evaluated included microporosity, mechanical strength and morphology. SEM analyses showed that the scaffolds did have uniform porosity with pore sizes in the range 50–250 μm. These pores were interconnected and distributed in 3D networks throughout the scaffolds. The increase of mechanical property values with increase in the wt% of CS/CMC was determined to be statistically significant. These observations support the effectiveness of this new approach to prepare tissue-engineered scaffolds. *In vitro* cytotoxicity studies showed that these scaffolds are nontoxic and can provide adequate support for cell growth and proliferation. The chitosan-MgG hybrid scaffold mimicked the ECM of natural tissue physically and chemically, and possessed high surface area, porosity, pore interconnectivity, and excellent mechanical stability.

Acknowledgments

This work is supported financially by the National Science Foundation through Engineering Research Center for Revolutionizing Metallic Biomaterials (ERC-0812348) and Nanotechnology Undergraduate Education (NUE-1242139).

Appendix A. Supplementary data

Supplementary data related to this article can be found at http://dx.doi.org/10.1016/j.bioactmat.2016.11.003.

Conflicts of interest

The authors declare no conflict of interest.

References

[1] A.S. Greenwald, et al., Bone-graft substitutes: facts, fictions, and applications, J. Bone Jt. Surg. Am. 83-A (Suppl 2) (2001) 98–103. Pt 2.
[2] T.E. Mroz, et al., Musculoskeletal allograft risks and recalls in the United States, J. Am. Acad. Orthop. Surg. 16 (10) (2008) 559–565.
[3] K.C. Kavya, et al., Fabrication and characterization of chitosan/gelatin/nSiO2 composite scaffold for bone tissue engineering, Int. J. Biol. Macromol. 59 (2013) 255–263.
[4] R. Langer, J.P. Vacanti, Tissue engineering, Science 260 (5110) (1993) 920–926.
[5] N.P. Rijal, U. Adhikari, N. Bhattarai, Magnesium incorporated polycaprolactone-based composite nanofibers, in: ASME 2015 International Mechanical Engineering Congress and Exposition, American Society of Mechanical Engineers, 2015.
[6] Z.S. Thompson, et al., Synthesis of keratin-based nanofiber for biomedical engineering, Jove.J. Vis. Exp. 108 (2016).
[7] K.E. Tanner, Bioactive composites for bone tissue engineering, Proc. Inst. Mech. Eng. H. 224 (12) (2010) 1359–1372.
[8] K. Whang, et al., Engineering bone regeneration with bioabsorbable scaffolds with novel microarchitecture, Tissue Eng. 5 (1) (1999) 35–51.
[9] C. Zhang, et al., A study on a tissue-engineered bone using rhBMP-2 induced periosteal cells with a porous nano-hydroxyapatite/collagen/poly(L-lactic acid) scaffold, Biomed. Mater 1 (2) (2006) 56–62.
[10] K.A. Hing, et al., Mediation of bone ingrowth in porous hydroxyapatite bone graft substitutes, J. Biomed. Mater Res. A 68 (1) (2004) 187–200.
[11] W. Bonfield, et al., Hydroxyapatite reinforced polyethylene–a mechanically compatible implant material for bone replacement, Biomaterials 2 (3) (1981) 185–186.
[12] L.J. Bonderer, A.R. Studart, L.J. Gauckler, Bioinspired design and assembly of platelet reinforced polymer films, Science 319 (5866) (2008) 1069–1073.
[13] N. Bhattarai, J. Gunn, M. Zhang, Chitosan-based hydrogels for controlled, localized drug delivery, Adv. Drug Deliv. Rev. 62 (1) (2010) 83–99.
[14] R.-H. Chen, et al., Advances in chitin/chitosan science and their applications, Carbohydr. Polym. 84 (2) (2011) 695.
[15] Y. Zhang, M.Q. Zhang, Synthesis and characterization of macroporous chitosan/calcium phosphate composite scaffolds for tissue engineering, J. Biomed. Mater. Res. 55 (3) (2001) 304–312.
[16] Y. Zhang, et al., Calcium phosphate-chitosan composite scaffolds for bone tissue engineering, Tissue Eng. 9 (2) (2003) 337–345.
[17] S. Khanal, et al., pH-responsive PLGA nanoparticle for controlled payload delivery of diclofenac sodium, J. Funct. Biomater. 7 (3) (2016) 21.
[18] N. Siddiqui, K. Pramanik, Development of fibrin conjugated chitosan/nano β-TCP composite scaffolds with improved cell supportive property for bone tissue regeneration, J. Appl. Polym. Sci. 132 (9) (2015) (p. n/a-n/a).
[19] C.S. Anast, et al., Evidence for parathyroid failure in magnesium deficiency, Science 177 (4049) (1972), 606-&.
[20] H. Zreiqat, et al., Mechanisms of magnesium-stimulated adhesion of osteoblastic cells to commonly used orthopaedic implants, J. Biomed. Mater. Res. 62 (2) (2002) 175–184.
[21] R.C. Zeng, et al., In vitro corrosion and cytocompatibility of a microarc oxidation coating and poly(L-lactic acid) composite coating on Mg-1Li-1Ca alloy for orthopedic implants, Acs Appl. Mater. Interfaces 8 (15) (2016) 10014–10028.
[22] S.M. Albelda, C.A. Buck, Integrins and other cell-adhesion molecules, Faseb J. 4 (11) (1990) 2868–2880.
[23] J. Gailit, E. Ruoslahti, Regulation of the fibronectin receptor affinity by divalent-cations, J. Biol. Chem. 263 (26) (1988) 12927–12932.
[24] G. Bazzoni, et al., Monoclonal-antibody 9eg7 defines a novel Beta(1) integrin epitope induced by soluble ligand and manganese, but inhibited by calcium, J. Biol. Chem. 270 (43) (1995) 25570–25577.
[25] M.P. Staiger, et al., Magnesium and its alloys as orthopedic biomaterials: a review, Biomaterials 27 (9) (2006) 1728–1734.
[26] M.P. Hage, G. El-Hajj Fuleihan, Bone and mineral metabolism in patients undergoing Roux-en-Y gastric bypass, Osteoporos. Int. 25 (2) (2014) 423–439.
[27] S.M. Rahman, et al., Synthesis and characterization of magnesium gluconate contained poly(lactic-co-glycolic acid)/chitosan microspheres, Mater. Sci. Eng. B Adv. Funct. Solid-State Mater. 203 (2016) 59–66.
[28] A. Edwards, et al., Poly(epsilon-caprolactone)/keratin-based composite nanofibers for biomedical applications, J. Biomed. Mater Res. B Appl. Biomater. 103 (1) (2015) 21–30.
[29] M.A. Aronow, et al., Factors that promote progressive development of the osteoblast phenotype in cultured fetal-rat calvaria cells, J. Cell. Physiol. 143 (2) (1990) 213–221.
[30] S.K.L. Levengood, M.Q. Zhang, Chitosan-based scaffolds for bone tissue engineering, J. Mater. Chem. B 2 (21) (2014) 3161–3184.
[31] R.J. Kroeze, et al., Biodegradable polymers in bone tissue engineering, Materials 2 (3) (2009) 833–856.
[32] L.Y. Jiang, Y.B. Li, C.D. Xiong, Preparation and biological properties of a novel composite scaffold of nano-hydroxyapatite/chitosan/carboxymethyl cellulose for bone tissue engineering, J. Biomed. Sci. 16 (2009).
[33] Z.S. Li, et al., Chitosan-alginate hybrid scaffolds for bone tissue engineering, Biomaterials 26 (18) (2005) 3919–3928.
[34] J. Venkatesan, et al., Chitosan-amylopectin/hydroxyapatite and chitosan-chondroitin sulphate/hydroxyapatite composite scaffolds for bone tissue engineering, Int. J. Biol. Macromol. 51 (5) (2012) 1033–1042.
[35] R.S. Tigli, A. Karakecili, M. Gumusderelioglu, In vitro characterization of chitosan scaffolds: influence of composition and deacetylation degree, J. Mater. Sci. Mater. Med. 18 (9) (2007) 1665–1674.
[36] S.V. Madihally, H.W.T. Matthew, Porous chitosan scaffolds for tissue engineering, Biomaterials 20 (12) (1999) 1133–1142.
[37] J.S. Mao, et al., Structure and properties of bilayer chitosan-gelatin scaffolds, Biomaterials 24 (6) (2003) 1067–1074.
[38] J. Wang, et al., Recommendation for modifying current cytotoxicity testing standards for biodegradable magnesium-based materials, Acta Biomater. 21 (2015) 237–249.
[39] L.Y. He, et al., Effect of magnesium ion on human osteoblast activity, Braz. J. Med. Biol. Res. 49 (7) (2016).
[40] T.Y. Nguyen, et al., Effects of magnesium on growth and proliferation of human embryonic stem cells, Conf. Proc. IEEE Eng. Med. Biol. Soc. 2012 (2012) 723–726.
[41] P.B. ODonnell, J.W. McGinity, Preparation of microspheres by the solvent evaporation technique, Adv. Drug Deliv. Rev. 28 (1) (1997) 25–42.